

# Qutrit state engineering with biphotons

Yu.I.Bogdanov

*Russian Control System Agency, "Angstrom", Moscow 124460 Russia.*

M.V.Chekhova, S.P.Kulik, G.A.Maslennikov, A.A.Zhukov.

*Department of Physics, Moscow M.V. Lomonosov State University, 119992 Moscow, Russia.\**

C.H.Oh, M.K.Tey

*Department of Physics, Faculty of Science, National University of Singapore, 117542 Singapore.*

(Dated: July 10, 2018)

The novel experimental realization of three-level optical quantum systems is presented. We use the polarization state of biphotons to generate a specific sequence of states that are used in the extended version of BB84 QKD protocol. We experimentally verify the orthogonality of the basic states and demonstrate the ability to easily switch between them. The tomography procedure is employed to reconstruct the density matrices of generated states.

PACS numbers: 42.50.-p, 42.50.Dv, 03.67.-a

The art of quantum state engineering, i.e., the ability to generate, transmit and measure quantum systems is of great importance in the emerging field of quantum information technology. A vast majority of protocols relying on the properties of two-level quantum systems (qubits) were introduced and experimentally realized. But naturally, there arose a question of an extension of dimensionality of systems used as information carriers and the new features that this extension can offer. The simplest extension provokes the usage of three-state quantum systems (qutrits). Recently new quantum key distribution (QKD) protocols were proposed that dealt specifically with qutrits [1, 2] and the eavesdropping analysis showed that this systems were more robust against specific classes of eavesdropping attacks [3, 4]. The other advantage of using multilevel systems is their possible implementation in the fundamental tests of quantum mechanics [5], giving more divergence from classical theory. The usage of multilevel systems also provides a possibility to introduce very specific protocols, which cannot be implemented with the help of qubits such as Quantum Bit Commitment, for example [6]. Recent experiments on realization of qutrits rely on several issues. In one case, the interferometric procedure is used, where entangled qutrits are generated by sending an entangled photon pair through a multi-armed interferometer [7]. The number of arms defines the dimensionality of the system. Other techniques rely on the properties of orbital angular momentum of single photons [6, 8, 9] and on postselection of qutrits from four-photon states [10]. Unfortunately all mentioned techniques provide only a partial control over a qutrit state. For example in a method, mentioned in [6, 8, 9] a specific hologram should be made for given qutrit state. The real parts of the amplitudes of a qutrit, generated in [7] are fixed by a characteristics of a fiber tritter, making it hard to switch between the states. Besides, in this method no tomographic control

over generated state had been yet performed.

In this paper we report the experimental realization of arbitrary qutrit states that exploits the polarization state of single-mode biphoton field. This field consists of pairs of correlated photons, is most easily obtained with the help of spontaneous parametric down-conversion (SPDC). By saying "single-mode" we mean that twin photons forming a biphoton have equal frequencies and propagate along the same direction. A pure polarization state of such field can be written as the following superposition of three basic states.

$$|\Psi\rangle = c_1|2, 0\rangle + c_2|1, 1\rangle + c_3|0, 2\rangle = c_1|\alpha\rangle + c_2|\beta\rangle + c_3|\gamma\rangle, \quad (1)$$

where  $c_i = |c_i|e^{i\phi_i}$  are complex probability amplitudes. The states  $|2, 0\rangle$  and  $|0, 2\rangle$  correspond to type I phase-matching where twin photons have collinear polarization vectors (for example, state  $|2, 0\rangle$  corresponds to two photons being in horizontal  $H$  polarization mode), and state  $|1, 1\rangle$  is obtained via type II phase-matching, where photons are polarized orthogonally (say, one of them is in  $H$  and the other one is in  $V$  mode). There exists an alternative representation of state  $|\Psi\rangle$  that maps the state onto the surface of the Poincare sphere [11]

$$|\Psi\rangle = \frac{a^\dagger(\theta, \phi)a^\dagger(\theta', \phi')|vac\rangle}{\|a^\dagger(\theta, \phi)a^\dagger(\theta', \phi')|vac\rangle\|}, \quad (2)$$

where  $a^\dagger(\theta, \phi)$  and  $a^\dagger(\theta', \phi')$  are the creation operators of a photon in a certain polarization mode  $a^\dagger(\theta, \phi) = \cos(\theta/2)a^\dagger + e^{i\phi}\sin(\theta/2)b^\dagger$ ,  $a^\dagger, b^\dagger$  are photon creation operators in correspondingly horizontal and vertical polarization modes,  $\theta \in [0, \pi]$ ,  $\phi \in [0, 2\pi]$  are polar and azimuthal angles that define the position of each photon on the surface of a sphere. The values of the angles can be calculated using the amplitudes and the phases of  $c_i$ . The operational orthogonality criterion for the polarization states of single-mode biphotons was proposed in [12] and experimentally verified in [13]. According

to the orthogonality criterion for biphoton polarization states, two polarization states  $\Psi_a$  and  $\Psi_b$  are orthogonal if one observes zero coincidence rate in the Brown-Twiss scheme, provided that the state  $\Psi_a$  is at the input, and polarization filters in each arm are tuned to assure maximal transmittance of each photon forming the state  $\Psi_b$  (set state). The goal of our work was to demonstrate the ability to prepare any given polarization state  $|\Psi\rangle$  and as a straightforward and practical example of given states, we chose the specific sequence that was presented in [1]. This sequence of 12 states forms four mutually unbiased bases with three states in each, and can be used in an extended version of BB84 QKD protocol for qutrits. The 12 states are defined in Table I.

State	$ c_1\rangle$	$ c_2\rangle$	$ c_3\rangle$	$\phi_1$	$\phi_2$	$\phi_3$
$ \alpha\rangle$	1	0	0	0	0	0
$ \beta\rangle$	0	1	0	0	0	0
$ \gamma\rangle$	0	0	1	0	0	0
$ \alpha'\rangle$	$\frac{1}{\sqrt{3}}$	$\frac{1}{\sqrt{3}}$	$\frac{1}{\sqrt{3}}$	0	0	0
$ \beta'\rangle$	$\frac{1}{\sqrt{3}}$	$\frac{1}{\sqrt{3}}$	$\frac{1}{\sqrt{3}}$	0	$120^\circ$	$-120^\circ$
$ \gamma'\rangle$	$\frac{1}{\sqrt{3}}$	$\frac{1}{\sqrt{3}}$	$\frac{1}{\sqrt{3}}$	0	$-120^\circ$	$120^\circ$
$ \alpha''\rangle$	$\frac{1}{\sqrt{3}}$	$\frac{1}{\sqrt{3}}$	$\frac{1}{\sqrt{3}}$	$120^\circ$	0	0
$ \beta''\rangle$	$\frac{1}{\sqrt{3}}$	$\frac{1}{\sqrt{3}}$	$\frac{1}{\sqrt{3}}$	0	$120^\circ$	0
$ \gamma''\rangle$	$\frac{1}{\sqrt{3}}$	$\frac{1}{\sqrt{3}}$	$\frac{1}{\sqrt{3}}$	0	0	$120^\circ$
$ \alpha'''\rangle$	$\frac{1}{\sqrt{3}}$	$\frac{1}{\sqrt{3}}$	$\frac{1}{\sqrt{3}}$	$-120^\circ$	0	0
$ \beta'''\rangle$	$\frac{1}{\sqrt{3}}$	$\frac{1}{\sqrt{3}}$	$\frac{1}{\sqrt{3}}$	0	$-120^\circ$	0
$ \gamma'''\rangle$	$\frac{1}{\sqrt{3}}$	$\frac{1}{\sqrt{3}}$	$\frac{1}{\sqrt{3}}$	0	0	$-120^\circ$

TABLE I: 12 states used in qutrit QKD protocol

The preparation part of our setup (Fig. 1) is built on the base of a balanced Mach-Zehnder interferometer (MZI) [14]. The pump part consists of frequency doubled "Co-

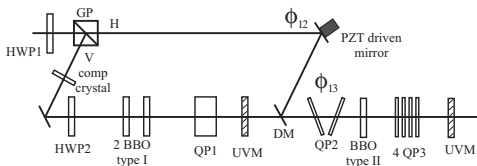


FIG. 1: Experimental setup (preparation part)

herent Mira 900" femtosecond laser, operated at central wavelength of 800 nm, 75 MHz repetition rate and with a pulse width of 100 fs, average pump power was 20 mW. The Glan-Tompson prism (GP), transmitting the horizontally polarized fraction of the UV pump and reflecting the vertically polarized fraction, serves as an input mirror of MZI. The reflected part, after passing the compensation BBO crystal and a half-wave plate (HWP2), pumps two consecutive 1 mm thick type-I BBO crystals

whose optical axis are oriented perpendicularly with respect to each other. The biphotons from these crystals pass through a 10 mm quartz plate (QP1) that serves as a compensator, and the pump is reflected by an UV mirror. Then the biphotons arrive at a dichroic mirror (DM) that is designed to transmit them and to reflect the horizontally polarized component of the pump coming from the upper arm of MZI. A piezoelectric translator (PZT) was used to change the phase shift of the horizontal component of the pump with respect to the one propagating in the lower arm. The UV beam, reflected from DM serves as a pump for 1 mm thick type-II BBO crystal. Two 1 mm quartz plates (QP2) can be rotated along the optical axis to introduce a phase shift between horizontally and vertically polarized type-I biphotons, and a set of four 1 mm thick quartz plates (QP3) serves to compensate the group velocity delay between orthogonally polarized photons during their propagation in type II BBO crystal. The measurement setup (Fig. 2) consists of a Brown-Twiss scheme with a non-polarizing 50/50 beamsplitter; each arm contains consecutively placed quarter- and half waveplates and an analyzer that was set to transmit the vertical polarization. This sequence of waveplates and

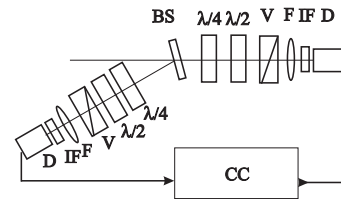


FIG. 2: Experimental setup (measurement part)

analyzer is referred to as a polarization filter. Interference filters of 5 nm bandwidth, centered at 800 nm and pinholes are used for spectral and spatial modal selection of biphotons. We use EGG-SPCM-AQR-15 single photon counting modules as our detectors (D1 and D2). We should mention, that due to the low pump power, the stimulated processes in our setup are negligibly small and only pairs of photons have been generated. The measurement of the generated states is done using the tomography protocol that was developed for polarization qutrits [16]. In order to reconstruct the density matrix of the measured state (which is generally mixed) one has to perform nine projective measurements of the fourth-order moments of the field for different settings of polarization filters. Polarization density matrix can be defined in the following way in terms of these moments [16, 17].

$$\begin{aligned}
 2\rho_{11} &= \langle a^{\dagger 2} a^2 \rangle, & \sqrt{2}\rho_{21} &= \langle a^{\dagger 2} ab \rangle, \\
 2\rho_{33} &= \langle b^{\dagger 2} b^2 \rangle, & \sqrt{2}\rho_{32} &= \langle a^{\dagger} b^{\dagger} b^2 \rangle, \\
 \rho_{22} &= \langle a^{\dagger} b^{\dagger} ab \rangle, & 2\rho_{31} &= \langle a^{\dagger 2} b^2 \rangle.
 \end{aligned} \tag{3}$$

This configuration of the measurement setup (Fig. 2) allows us to verify the orthogonality of the states that belong to the same basis.

**Compensation.** In order to have the three terms in superposition (1) interfering, one must achieve their perfect overlap in frequency, momentum and time domains. From the experimental point of view this means that the biphoton wavepackets coming from the two type I crystals and from the type II crystal must be overlapped. The overlap in the frequency domain is achieved by the usage of 5nm bandwidth interference filters and the overlap in momentum is ensured by using pinholes that select one spatial mode of the biphoton field. But the overlap in time cannot be achieved easily when using a pulsed laser source, because it is necessary to compensate for all the group delays that biphoton wavepackets acquire during their propagation through the optical elements of the setup [15]. It was found that in order to overlap type-I biphotons with type-II, the pump pulse from the lower arm must be delayed. In our case the value of the delay is 50 ps. This was achieved by inserting an additional 2 mm BBO crystal in the lower arm. The overlap between the states  $|2, 0\rangle$  and  $|0, 2\rangle$  was achieved by inserting a 10 mm quartz plate directly after the two type I BBO crystals. After overlapping the biphotons with these techniques, the average coincidence count rate that we observed was of about 1 Hz. The high visibility of interference patterns that we obtained was a criterion for a good compensation.

**Experimental procedure.** In order to create a given qutrit state we needed to have independent control over four real parameters - two relative amplitudes and two relative phases. In the experiment we used HWP1 to control the amplitude of the state  $|1, 1\rangle$ , and HWP2 to control the relative amplitudes of the states  $|2, 0\rangle$  and  $|0, 2\rangle$ . The relative phase  $\phi_{13} = \phi_3 - \phi_1$  between the states  $|2, 0\rangle$  and  $|0, 2\rangle$  can be controlled with the help of rotating quartz plates (QP2). The relation of the phase  $\phi_{12} = \phi_2 - \phi_1$  between the state  $|\Psi'\rangle = |2, 0\rangle + e^{i\phi_{13}}|0, 2\rangle$  and  $|1, 1\rangle$  to the voltage applied to PZT can be found by monitoring the pump interference pattern in M-Z interferometer. We found that the change of voltage by 1 V resulted in the phase shift of  $51.7^\circ$  and  $\phi_{12}$  grew linearly with the applied voltage.

States that constitute the first basis are trivial (Table I). They can be produced with the help of a single crystal, corresponding to type I or type II interaction. State  $|2, 0\rangle$  is generated when first  $\lambda/2$  (HWP1) angle corresponds to the maximal reflection of the pump beam into the lower arm of a Mach-Zehnder and the angle of the second half-lambda waveplate (HWP2) is equal to  $0^\circ$ . In order to generate state  $|0, 2\rangle$ , the HWP2 must be rotated by  $45^\circ$  degrees from  $0^\circ$ , and to generate state  $|1, 1\rangle$  the HWP1 is rotated such, that the whole pump goes into the upper arm of Mach-Zehnder. Therefore, in the following, we will consider only the generation of the rest nine states, i.e. those forming the other three bases. According to Table I, only the relative phases between the basic states are to be varied. This allows us to use the same settings

of the HWP's for the generation of nine states. It is also convenient to perform three sets of data acquisition - for the fixed  $\phi_{13}$  values of  $0, +120^\circ$  and  $-120^\circ$ , we change  $\phi_{12}$  values in the range of, say, few periods and perform all tomographic measurements for each value of the phase  $\phi_{12}$ . Then we select the values of  $\phi_{12}$  that correspond to the generation of the required state. For example, in order to generate the state  $\beta'$ , we use  $\phi_{13} = -120^\circ$  and  $\phi_{12} = 120^\circ$ . The values of the moments at this point allow us to restore a raw density matrix of the generated state and compare it to the theoretical value.

The following procedure was used in order to verify the orthogonality of the states that form a certain basis. First we chose a set state to which we would tune our polarization filters. Then the values of the angles of quarter- and half- waveplates (Fig. 2) ( $\chi_1, \theta_1, \chi_2, \theta_2$ ) that assure the maximal projection of the polarization state of each photon on the  $V$  direction can be calculated by mapping the set state on the Poincare sphere. Here, the lower index "1" corresponds to the transmitted arm, and the index "2" to the reflected arm of BS. We chose states  $|\alpha'\rangle$ ,  $|\alpha''\rangle$  and  $|\alpha'''\rangle$  to be our set states for each basis. Then, by setting the phase  $\phi_{13}$  fixed and by varying the phase  $\phi_{12}$  we measured the number of coincidence counts that correspond to the certain fourth order moment of the field. According to the orthogonality criterion, the coincidence rate should fall to zero when the values of  $\phi_{13}$  and  $\phi_{12}$  correspond to the generation of the states orthogonal to the set ones.

**Results and discussion.** Let us consider the generation of the state  $|\beta''\rangle$ . In this case  $\phi_{13} = 0, \phi_{12} = 120$ . In Fig. 3 the measured values of the real and imaginary parts of the density matrix components  $\rho_{21}$  and  $\rho_{32}$  on phase  $\phi_{12}$  are shown as function of the phase  $\phi_{12}$ . The number of accidental coincidences was negligibly small and was not subtracted in data processing.

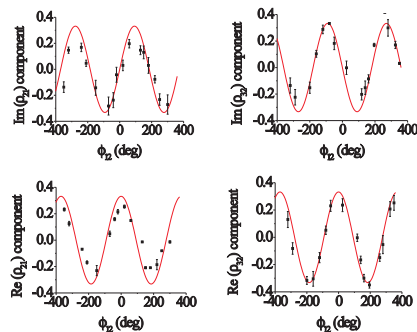


FIG. 3: Imaginary and real values of non-diagonal density matrix components used to reconstruct state  $|\beta''\rangle$ . Theoretical dependence is plotted with a solid curve.

The phase  $\phi_{13} = 0$  remained constant during the tomography procedure. After obtaining the dependence of the moments  $\rho_{21}$  and  $\rho_{32}$  on phase  $\phi_{12}$  we fitted our data

with theoretical dependencies, using the least-square approximation method. The obtained values of all components were substituted in Eq. 3. The obtained density matrix for state  $|\beta''\rangle$  is given below.

$$\rho_{\beta''} = \begin{pmatrix} 0.355 & -0.054 - 0.210i & 0.315 - 0.010i \\ -0.054 + 0.210i & 0.340 & -0.106 + 0.262i \\ 0.315 + 0.010i & -0.106 - 0.262i & 0.305 \end{pmatrix} \quad (4)$$

The eigenvalues of this matrix are  $\lambda_1 = 0.877, \lambda_2 = 0.136, \lambda_3 = -0.013$ . A corresponding set of eigenvectors is  $X = (0.587, -0.173 + 0.521i, 0.594 - 0.071i)$ ;  $Y = (0.642, 0.379 - 0.649i, 0.048 + 0.143i)$ ;  $Z = (0.493, -0.287 + 0.224i, -0.769 - 0.178i)$ . Although the density matrix (Eq. 4) is Hermitian and the condition  $Tr(\rho) = 1$  is satisfied, it doesn't correspond to any physical state because of the negativity of one of the eigenvalues. We want to point out that a first main component  $(\rho_{exp}^1)_{ij} = X_i X_j^*$  of a considered density matrix, which has a weight 0.878 is already close to the theoretical state vector  $|\beta''\rangle$  and the corresponding fidelity is  $F = Tr(\rho_{th} \rho_{exp}^1) = 0.9903$ . The other two components correspond to the "experimental noise" that is due mainly to misalignments of a setup and small volume of collected data. Even at this point, the obtained raw fidelity values show the high quality of a generated state. We have obtained similar eigenvalues for all other states and raw fidelity computed for the main density matrix component as described above have varied from 0.983 to 0.998. We also employed the maximum likelihood method of quantum state root estimation (MLE) [16, 18] to make a tomographically reconstructed matrix satisfy its physical properties, such as positivity. The results are presented in the following table (Table II). The level of statistical fluctuations in fidelity estimation was determined by the finite size of registered events ( $\sim 500$ ). All experimental fidelity values lie within the theoretical range of 5% ( $F = 0.9842$ ) and 95% ( $F = 0.9991$ ) quantiles [16, 19].

State	$F_{MLE}$	State	$F_{MLE}$	State	$F_{MLE}$
$ \alpha'\rangle$	0.9989	$ \alpha''\rangle$	0.9967	$ \alpha'''\rangle$	0.9883
$ \beta'\rangle$	0.9967	$ \beta''\rangle$	0.9989	$ \beta'''\rangle$	0.9989
$ \gamma'\rangle$	0.9883	$ \gamma''\rangle$	0.9883	$ \gamma'''\rangle$	0.9967

TABLE II: Fidelities estimated with Maximum Likelihood Method

The obtained fidelity values show the high quality of the prepared states. Altogether with the high visibility of the interference patterns that we obtained, we can conclude that our technique for the preparation of

qutrits is quite reliable. The other test of the quality of prepared states is the fulfillment of the orthogonality criterion for the states that belong to the same basis. For each set state we calculated the settings of waveplates in our measurement setup that ensured the maximal projection of each photon on the vertical polarization direction. In Fig. 4 we show the dependence of the coincidence rate for the following setting of waveplates  $\chi_1 = 28.3^\circ, \theta_1 = -33.5^\circ, \chi_2 = -24^\circ, \theta_2 = -2^\circ$ . These

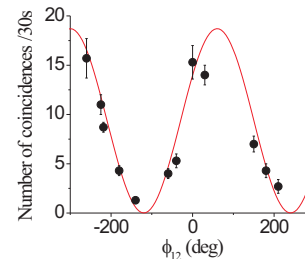


FIG. 4: Dependence of number of coincidences on a phase  $\phi_{12}$  for a given settings of polarization filters.

values correspond to the set state  $|\alpha'''\rangle$ . As one can see, for the fixed value  $\phi_{13} = 0$  the coincidence rate is almost equal to zero, when phase  $\phi_{12} = -120^\circ$ . This corresponds to the generation of the state  $|\beta''\rangle$ , which is orthogonal to  $|\alpha'''\rangle$ . The visibility of this pattern is equal to 93.2%. For the other bases, the obtained values of visibilities varied from 92% to 95%. With these values of visibility, the lowest value of coincidence rate corresponds to the accidental (Poissonian) coincidence level and therefore the obtained data verifies the orthogonality criterion.

**Conclusions.** We realized an interferometric method of preparing the three-level quantum optical systems, that relied on the polarization properties of single-mode two-photon light. The specific sequence of states was generated and measured with high fidelity values. The orthogonality of the states that form mutually unbiased bases was experimentally verified. As an advantage of this method we note that all control of the amplitudes and phases of each basic state in superposition (1) is done using linear optical elements, making it easy to switch from one state to another and providing the full control over the state (1). The main disadvantage is that we cannot generate an entangled qutrits in this configuration. Our setup also allows one to prepare an arbitrary polarization qutrit state on demand.

**Acknowledgments.** Useful discussions with A.Ekert, B.Englert, D.Kazlikowski, C.Kurtsiefer, L.C.Kwek, A.Lamas-Linares and A.Penin are gratefully acknowledged. This work was supported in part by Russian Foundation of Basic Research (projects 03-02-16444 and 02-02-16843) and the National University of Singapore's Eastern Europe Research Scientist and Student Pro-

gramme.

---

\* Electronic address: postmast@qopt.phys.msu.su

- [1] H.Bechmann-Pasquinucci, A.Peres, Phys. Rev. Lett. **85**, 3313 (2000).
- [2] D.Kaszlikowski, *et al*, Phys. Rev.A. **67** 012310 (2003).
- [3] D.Bruss, C.Machiavello, Phys. Rev. Lett. **88**, 127901 (2002).
- [4] T.Durt, *et al*, Phys. Rev.A. **67**, 012311 (2003).
- [5] D.Collins, *et al*, Phys. Rev. Lett. **88**, 040404 (2002).
- [6] N.Langford, *et al*, Phys. Rev. Lett. **93**, 053601 (2004).
- [7] R.T.Thew, *et al*, Quantum Information and Computation, Vol.4, No.2, 93 (2004).
- [8] A.Vaziri, *et al*, Phys. Rev. Lett. **91**, 227902 (2003).
- [9] G.Molina-Terriza, *et al*, quant-ph/0401183.
- [10] J.C.Howell, *et al*, Phys. Rev. Lett. **88**, 030401 (2002).
- [11] A.V.Burlakov and M.V.Chekhova, Sov. JETP. **75**, 8, 432 (2002).
- [12] M.V.Chekhova, *et al*, Sov. JETP Letters. **76** (10), 696 (2002).
- [13] M.V.Chekhova, *et al*, quant-ph/0311005.
- [14] G.A.Maslennikov, *et al*, Journal of Optics B. **5**, 530 (2003).
- [15] Y-H.Kim, *et al*, Phys. Rev.A. **61**, 051803(R) (2001).
- [16] Yu.I.Bogdanov, *et al*, Phys. Rev. A. **70**, 042303 (2004)
- [17] D.N.Klyshko, JETP 84, 1065 (1997).
- [18] Yu.I.Bogdanov, *et al*, JETP Lett. **78**, N6. p.352-357 (2003).
- [19] The 5% and 95% quantiles cuts the left and right tail of distribution correspondingly.